

PAPER • OPEN ACCESS

Real-space imaging of several molecular layers of C_{60} in the rotational glass phase

To cite this article: Michael Marz *et al* 2023 *J. Phys.: Condens. Matter* **35** 405004

View the [article online](#) for updates and enhancements.

You may also like

- [\(Invited\) Multiple Photosynthetic Reaction Centers of Porphyrinic Polypeptide- \$Li^+\$ @ \$C_{60}\$ Supramolecular Complexes](#)
Kei Ohkubo, Tetsuya Hasegawa, Regis Rein *et al.*
- [\(Invited\) Lithium-Ion Endohedral Fullerenes on Carbon Nanotube Electrode-Laminated Perovskite Solar Cells As Dopants and Anti-Oxidants](#)
Il Jeon, Ahmed Shawky, Esko Kauppinen *et al.*
- [Molecular dynamics and structural phase transition in \$C_{60}\$ nanowhiskers](#)
Hideaki Kitazawa, Kenjiro Hashi, Tuerxun Wuernisha *et al.*

Real-space imaging of several molecular layers of C₆₀ in the rotational glass phase

Michael Marz¹ , Andrew Issac¹, Veronika Fritsch², Amina Kimouche³ 
and Regina Hoffmann-Vogel^{3,*} 

¹ Physikalisches Institut, Karlsruhe Institute of Technology, Wolfgang-Gaede-Str. 1, D-76128 Karlsruhe, Germany

² Experimental Physics VI, Center for Electronic Correlations and Magnetism, University of Augsburg, 86159 Augsburg, Germany

³ Department of Physics and Astronomy, University of Potsdam, 14476 Potsdam-Golm, Germany

E-mail: regina.hoffmann-vogel@uni-potsdam.de

Received 15 February 2023, revised 8 June 2023

Accepted for publication 27 June 2023

Published 10 July 2023



CrossMark

Abstract

C₆₀ is a model system to study molecule–surface interactions and phase transitions due to its high symmetry and strong covalent π bonding within the molecule versus weak van-der-Waals coupling between neighboring molecules. In the solid, at room temperature, the molecule rotates and behaves as a sphere. However, the pentagonal and hexagonal atomic arrangement imposes deviations from the spherical symmetry that become important at low temperatures. The orientation of the C₆₀ can be viewed to represent classic spins. For geometrical reasons the preferred orientation of neighboring C₆₀ cannot be satisfied for all of the neighboring molecules, making C₆₀ a model for disordered spin systems with frustration. We study several molecular layers of C₆₀ islands on highly oriented pyrolytic graphite using scanning tunneling microscopy at liquid nitrogen temperatures. By imaging several layers we obtain a limited access to the three-dimensional rotational structure of the molecules in an island. We find one rotationally disordered layer between two partially rotationally ordered layers with hexagonal patterns. This exotic pattern shows an example of the local distribution of order and disorder in geometrically frustrated systems. Scanning tunneling spectroscopy data confirms the weak interactions of neighboring molecules.

Supplementary material for this article is available [online](#)

Keywords: fullerene, orientational order, spin glass, frustration, scanning tunneling microscopy

(Some figures may appear in colour only in the online journal)

* Author to whom any correspondence should be addressed.



Original Content from this work may be used under the terms of the [Creative Commons Attribution 4.0 licence](#). Any further distribution of this work must maintain attribution to the author(s) and the title of the work, journal citation and DOI.

1. Introduction

After the invention of scanning tunneling microscopy (STM) it has first been used for imaging ordered structures that can be rather complex, such as the Si (111) 7×7 reconstruction [1]. Investigating ordered structures helps to understand contrast formation and to ensure reproducibility. However, STM is not limited to ordered structures. All members of the scanning probe microscopy (SPM) family are intended to image individual objects instead of using statistical averaging of large ensembles. This capability becomes particularly important for nanostructures, local defects and disordered structures [2–4]. Advanced techniques of the SPM family such as spin-polarized STM [5] become even more challenging on disordered structures. In particular for non-collinear structures where several spin orientations are present on the same surface the capability of spin-polarized STM to image individual nanostructures becomes decisive [6]. Usually, using SPM such structures are studied in two dimensions.

C_{60} is a prominent molecule with tunable electronic properties resulting in semiconducting, magnetic or superconducting behavior [7–11] and can be used for a wealth of chemical and nanotechnological applications such as a nanomechanically oscillating transistor [12], sensors and photovoltaic cells [13] or a quantum computer [14]. Of particular interest are the structural phases when adsorbed on surfaces and their electronic configurations [15–22]. Part of these are rotationally disordered [23]. Bulk structural studies have revealed that at room temperature C_{60} is crystallized in an fcc phase of Fm3m symmetry with individual molecules rotating by thermal activation [24, 28]. However, the pentagonal and hexagonal atomic arrangement imposes a deviation from spherical symmetry with an activation energy smaller than room temperature. The optimal orientation is such that a double-bond of one molecule (high electronic density—located between two hexagons) faces a pentagon of another molecule (low electronic density) [23].

At temperatures below 90–260 K, bulk C_{60} crystals show a rotationally predominantly ‘frozen’ state where the molecules can occupy two possible configurations corresponding to different local energy minima and shuffle (swing) between these two orientations [24, 25]. The orientations are separated by an energy barrier of 290 meV [26] and the molecule can swing between two equilibrium positions. Other publications do not provide a particular value for the energy barrier to explain the observed behavior [27]. Below 90 K even these swings are frozen in the bulk [24]. C_{60} undergoes a transition from a face-centered cubic Fm3m phase with rotational disorder observed at temperatures above about 260 K to a low-temperature phase with rotational order of the individual C_{60} molecules and with Pa3 symmetry [23, 28, 29, 31]. In the low temperature configuration, the symmetry is lowered when the four equivalent molecules located in the fcc bulk unit cell become inequivalent by fixing their orientation. For the (111) oriented bulk plane the molecules located on the corners of the cubic unit cell, i.e. the corners of triangles at the surface, display a three-fold axis in the direction perpendicular to the surface while the molecules located at the edges of the triangular unit cell

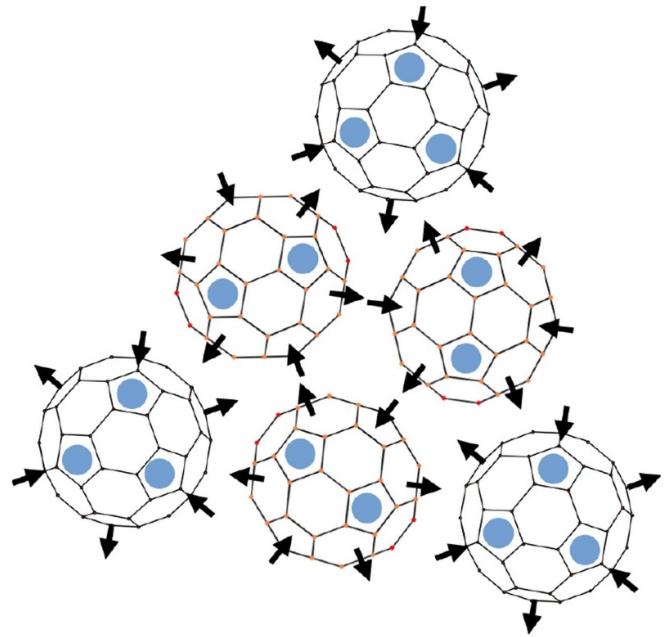


Figure 1. Model for a C_{60} surface layer at low temperatures when the rotation is locked. In empty-state STM images, mainly the pentagons, marked with blue circles, are imaged as bright. The arrows represent the electrostatic field in the surface plane. The orientation of the unit cell has been chosen in order to match the STM images shown below in figures 2 and 3. After [35].

(i.e. the ones located at the center of the faces of the cube) display a two-fold axis [27]. In the transition region between thermally-induced rotational hopping and the rotational frozen state, a glass transition has been observed, where the term ‘glass’ refers to the disordered rotational state of the molecules [29–31].

The intramolecular structure of C_{60} is visible on several substrates and typically gives rise to a bright and dim contrast [32–34]. The alignment described above for the bulk has also been found at surfaces and causes a 2×2 arrangement [35]. For a two-dimensional arrangement of C_{60} on the contrary a 1×1 lattice with all molecules pointing in the same direction has been found to be the energetically most favorable configuration [36, 37]. The orientation of C_{60} can be regarded as similar to a classic spin degree of freedom. For geometrical reasons the preferred relative orientation of neighboring C_{60} cannot be satisfied for all molecules, see figure 1, making C_{60} a model for disordered spin systems with frustration.

Here, we study the onset of orientational disorder near the glass transition of C_{60} molecular layers as a model for disordered spin systems. We show STM images of molecular islands on highly oriented pyrolytic graphite (HOPG) obtained at liquid nitrogen temperatures. We observe an internal structure on some of the molecules related to deviations from spherical symmetry while others show noise characteristic for swings. We observe a 2×2 molecular superstructure in C_{60} island that points to a freezing of the rotational degrees of freedom for part of the molecules. Since we observe the molecular internal structure on several molecular layers of one island, we can draw conclusions on the three-dimensional

rotational order of the island. Scanning tunneling spectra as a function of lateral position show a disordered structure of the molecular orbitals possibly influenced by the interactions of the molecules with the substrate.

2. Experimental methods

The experiments were conducted in a Omicron low temperature STM system with a base pressure lower than 1×10^{-8} Pa. We used macroscopic piece of grade H-HOPG with a mosaic spread of $3.5^\circ \pm 1.5^\circ$ as a substrate and mounted it on a contacted piece of Si attached to a sample holder suitable for direct current heating. We then cleaved the graphite using adhesive tape and introduced it immediately after cleavage into the ultrahigh vacuum chamber. All further preparation and measurement steps were conducted inside the vacuum chamber without ever exposing the sample to air. The sample was cleaned by running a current through the piece of Si in vacuum. The HOPG was heated to a temperature of 420–470 K. The pressure in the chamber was 3×10^{-9} Pa after cooling the sample to liquid nitrogen temperatures. The HOPG substrate surface cleanliness was checked at liquid nitrogen temperatures using STM within the same vacuum vessel. The samples were then removed from the STM and kept in a room-temperature environment for 30 min, an insufficient time to reach room temperature. We estimate the sample temperature to be around 200–230 K at the time of deposition also in relation to previous results [38]. C_{60} was deposited on the sample by thermal evaporation from a simple home-built evaporator consisting of a boron nitrate crucible heated by a tantalum foil. For additional details, see reference [39]. By varying the heating time of the evaporator between 1 min 30 s and 5 min while keeping the same heating current, the amount of C_{60} deposited on the sample was varied. The sample was then transferred into the pre-cooled STM and cooled again to liquid nitrogen temperatures for STM imaging. Imaging was performed using a Nanonis electronics. We used W tips prepared by electrochemical etching using a tip-etching tool from Omicron. The overall structure of the islands and the epitaxial relationship of the C_{60} to the HOPG substrate have been studied previously [39]. Many images were obtained showing individual local differences. For the data shown in figures 2 and 3, at least three images have been obtained on the same area that show similar resolution and similar internal structure of the molecules. In additional images we find both, a 2×2 ordered structure as discussed below and a disordered structure. In total at least 21 terraces have been imaged with high resolution under similar measurement conditions.

Scanning tunneling spectroscopy (STS) measurements were carried out on areas between 3×3 nm² and 5×5 nm². The spectra were generated by numerical differentiation of the I - V characteristics. The image resolution varied from 64×64 , and 100×100 to 128×128 pixels. For each pixel the bias voltage was varied from -3.5 V to 2 V or -2 V to 2 V while 128 or 256 spectral data points were recorded. In this way three-dimensional datasets were obtained. We expect

that contacting the sample through the piece of Si and performing the measurements at liquid nitrogen temperatures had an impact on the spectra in particular for negative voltages, where a Schottky barrier was active and the signal-to-noise ratio was reduced. We have acquired eight datasets in total. All showed qualitatively similar results. Two datasets with particularly good resolution were selected as examples for a more detailed data analysis—one for C_{60} located on a C_{60} island of at least three molecular layer height and one for C_{60} located directly on the HOPG surface. A Gaussian filter was used for noise suppression for the spectra.

For averaging the C_{60} on C_{60} spectra, first, starting from the topography images, a distorted hexagonal lattice was laid on top of the data to mark the area occupied by each molecule, reminiscent of Voronoi cells. Spectra obtained within one hexagon were considered to belong to one molecule. To identify spectra obtained on top of the molecules, we then took the following procedure because we found that it allowed to correctly identify molecules. The spectra were divided into two categories: spectra with four data points with values for the slope of more than 0.2 nA V⁻¹ within a window of -3.5 V to 3.2 V were flagged ‘on’ a molecule, those that did not fulfil the criterium were flagged ‘between’ molecules. Then the average was calculated for all spectra ‘on’ molecules. For the C_{60} on HOPG spectra a similar method was not successful, because even within one molecule the spectra differ from each other. Here, three molecules, labeled with numbers 1, 2 and 3, are chosen as examples to represent the dataset. For simplicity, the spectra acquired over each pixel were averaged separately within rectangular areas covering each molecule. For this procedure the shape and position of the rectangles could influence the overall appearance of the molecular spectra. However, the differences observed between molecules 1, 2 and 3, e.g. the presence or absence of peaks cannot only be explained by different averaging methods. The spectra are influenced not only by the orientation of the molecules but also by the position of the molecules with respect to the substrate carbon atoms. This relative position individually differs for each molecule on the image. Through this averaging procedure we avoid a possible loss of information by averaging out the individual peaks in spectra acquired above different molecules.

3. Results and discussion

3.1. STM images

To understand the orientational arrangement we have investigated C_{60} islands on a HOPG substrate using high-resolution STM. For large scale images of the islands, see reference [39]. HOPG provides a unique adsorption platform as an electronically inert substrate for C_{60} , optimizing the electronic coupling [40]. Figure 2(a) shows an overview of the molecules in a C_{60} island with molecular resolution obtained on several terraces named A, B and D. B is one layer higher compared to A, while D is two layers higher than B, layer C is not discussed here. There is an additional molecular layer below layer A.

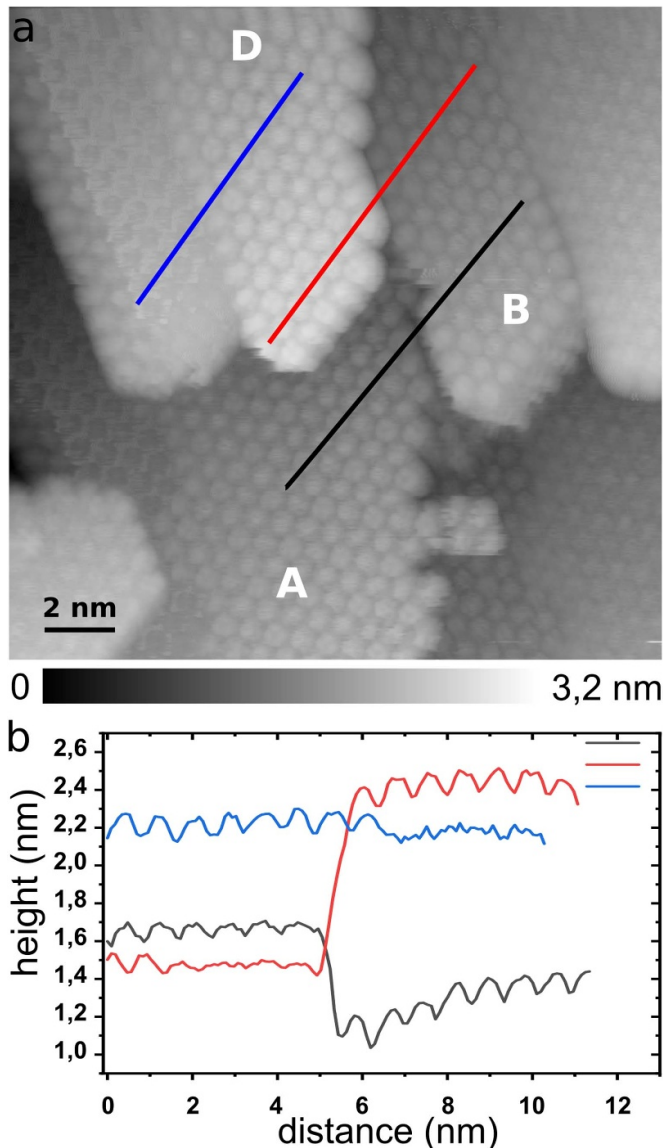


Figure 2. (a) High resolution image of C_{60} islands, $V_b = 2$ V and $I_t = 10$ pA. Three different terraces are marked with A, B and D. (b) Line-cuts through (a) along the lines marked in black, red and blue in (a). The direction of the line-cuts is from the upper right corner to the lower left corner. From these line-cuts the relative height of the different terraces can be measured.

The line profiles in figure 2(b) show that the height difference between the terraces is indeed one or two molecular layers, resp. To avoid confusion by the sample tilt, the line profiles have been taken along the same direction. C_{60} molecules appear as bright protrusions in the STM image and adopt a closely packed fcc (111) hexagonal surface growth mode, in spite of the lattice mismatch to the substrate lattice, indicating a weak molecule–substrate interaction as expected for the van-der-Waals interaction. The unit cell vectors of the lattice are each equal to 0.8 ± 0.1 nm. The formation of islands indicates that the intermolecular bonding is relatively strong compared to the molecule–substrate interaction. The intermolecular separation is close to the natural molecule–molecule distance of 1 nm observed in bulk C_{60} crystals [28].

Adsorption orientations of C_{60} can be distinguished in the intramolecular pattern shown as a close-up view in figures 3(a)–(c). These images are cut from a consecutively acquired image with respect to the one shown in figure 2(a), i.e. the terraces A, B and D are the same as the ones labeled in figure 2(a). The images have been smoothed by matrix averaging to highlight the molecular orientations that can be distinguished due to the molecule’s deviations from spherical symmetry. In addition, we report on noise due to molecular hops that occur during scanning. For unsmoothed images, see the supplementary material, section 1. To analyze the orientational ordering of the molecules in more detail, next to each image we draw the corresponding configurations of C_{60} molecules as models. For terraces A and D (figures 3(a) and (c)) we find many C_{60} molecules that show a three-fold contrast, i.e. an orientation exposing the frontier molecular orbital to the STM tip. This three-fold contrast is also observed on other areas of the surface, see the supplementary material, section 2.

Our STM images (figure 3(a)) for terrace A and terrace D in figure 3(c) clearly show that every fourth C_{60} molecule exhibits a three-fold contrast, forming the hexagonal arrangement of a (111) plane of the fcc close-packed structure with 2×2 reconstruction of the C_{60} lattice by orientational ordering of part of the molecules on terraces A and D. This gives rise to superstructure spots in the Fourier transform, see the supplementary material, section 3. In the literature, measured STM contrast of C_{60} molecule has been compared to calculations in order to identify the orientation of the molecule on the basis of the measured contrast. Each molecule shows deviations from spherical symmetry. It has been found that when a hexagon is oriented towards the STM tip, the appearance is threefold [35, 41]. The intermediate C_{60} molecules filling the spaces between these three-fold-oriented molecules often appear noisy in the raw data in figures 3(a) and (c). We can infer that in terrace A and D, long-range orientational correlations between neighboring molecules are established at this temperature leading to an ordered structure.

Remarkably, the rotational orientations of C_{60} are not random. Those with an orientation of the C_{60} molecule hexagon towards the tip show a periodic distribution in the terraces A and D derived from linear chains if the intermediate molecule is ignored. This distribution of hexagon states is typical for the disordered ground state of C_{60} [24, 25].

On terrace B (figure 3(b)) the molecules do not exhibit three-fold axes but a different symmetry of the molecular orbitals and the layer is rather rotationally disordered and some molecules appear noisy in the raw data due to swinging on the timescale of the measurement [42, 43]. At this temperature, we can assume that the rotational freedom of molecules is not fully lost. Instead of a fixed transition temperature between freezing and swinging, there is a broad range of transitions, because there is a random orientational environment of each molecule that leads to a not-well-defined energy barrier [44]. In addition, a rotational swinging of the molecules could be induced by the tunneling current [42, 43]. This should be studied by varying the imaging parameters. The random orientation of C_{60} molecules on terrace B as well as their rotational swinging points to a metastable state. No correlations

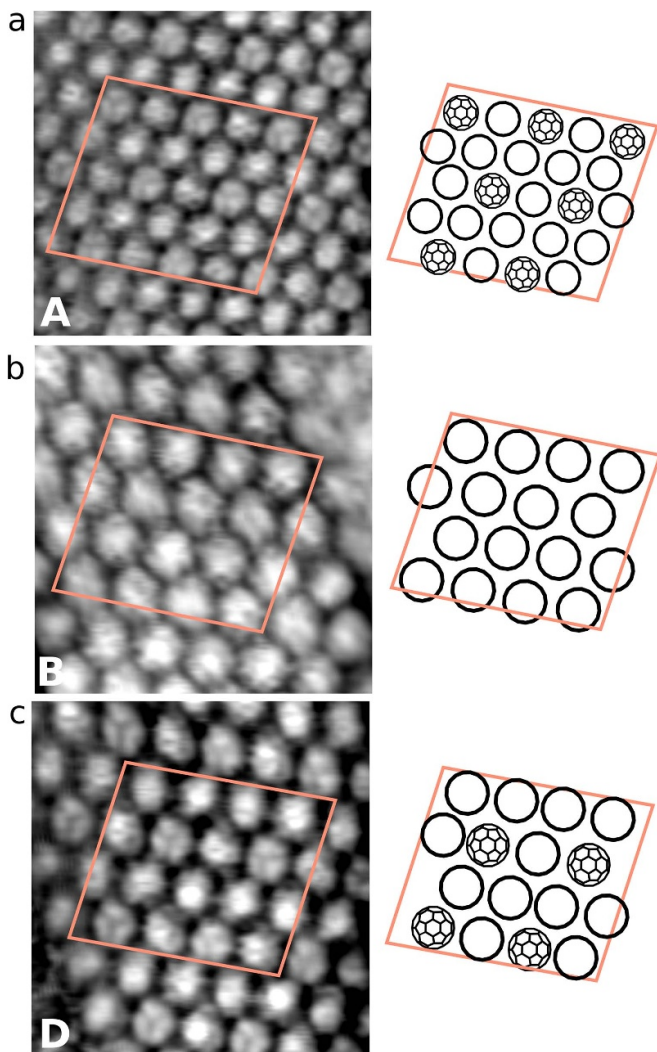


Figure 3. (a)–(c) High resolution images of C_{60} islands cut from layers A, B and D in figure 2, taken from a consecutive image, shown alongside the proposed structure obtained from a careful analysis of the images (a)–(c). Only molecules where the orientation is clearly identified are drawn in the schematics. The molecules showing a three-fold axes perpendicular to the sample surface are drawn with a hexagon on top of the molecule. There is a 2×2 superstructure related to differences in the molecular orientation in layers A and D while layer B does not show an orientational structure.

between individual orientations of neighboring C_{60} molecules have been found leaving the molecules locked in different orientations. Our data are in agreement with the assumption that the layer B exhibits a geometrical frustration of its orientational state: by frustration for part of the molecules it is not possible to reach the desired lowest-energy orientation, and they remain in the lowest energy state that they can possibly reach and the perfect symmetry is broken. By symmetry, usually there is another orientational state with similar energy that is separated by an energy barrier. If the thermal energy is sufficient to overcome the barrier, the molecules swing between the two states.

We attribute these differences to small variations in the nearest-neighbor intermolecular interactions between the first

and third layers. The bonding in layers A and D is different with respect to layer B. Since the bonding between layers is caused by long range van der Waals forces, the bonding is weak with not much selectivity in molecular ordering compared to stronger bonding [45, 46]. In our case, due to the large bonding distance, we can assume that the molecular order is only governed by nearest neighbor interactions. We relate the detection of no preferential orientation to intermolecular bonding.

We interpret the differences between the layers A, B and D from the overall appearance of the island: only in the top part of figure 2(a), the island and all three layers appear connected, in the lower part, they are disconnected. This can be evaluated from the figure 2(a) if the molecules along the blue line (top part of the image) and along the black line (bottom part of the image) are followed closely by eye. In addition, Fourier-transforms shown in the supplementary material, section 3, show small variations of the lattice constant between different layers. We have therefore additionally evaluated the molecular positions in direct space in the supplementary material, section 4. Since the layers result from an fcc crystal with abcabc-stacking along its (111) direction, and A and D are four layers apart, the molecules in A and D are expected to be located on top of each other. Figure S3 shows that this is clearly not the case. In addition, we have analyzed the structure of the layer below layer A, in the bottom right part of the image. This layer consists of two parts: on the left, the molecules are stable, on the right the molecules are swinging.

The structural differences between different parts of the image point to an intermolecular distance that varies across the image. Such partial island connections have been described in [37] and arise from strain in the island. The strain could result from several causes including inhomogeneities in the substrate as it is known that the C_{60} relates to the substrate [39, 47]. We conclude that the strain in the part of the island that contains layers A and D could be different from the strain in layer B resulting in different local energy barriers for swings and in a different degree of ordering and geometrical frustration. This observation can be generalized to the system of C_{60} -islands on HOPG if only the molecules exposing hexagons are considered: for figure 2, we observe two ordered layers and one disordered layer, a fraction of 67% of order for this temperature. For 21 terraces we have studied here, 14 have appeared ordered and 7 were interpreted to be disordered, a fraction of 67%. This can be compared to data from reference [28, 48], where the degree of the orientational order in C_{60} at low temperatures is studied using diffraction measurements, suggesting that about 30% of the structure is orientationally disordered even at 14 K associated with randomly oriented molecules.

3.2. STS measurements

In order to experimentally untangle the behavior of C_{60} molecular orbitals, we have acquired STS data in addition. Figure 4(a) shows an image taken on a C_{60} island of at least three molecular layers height where spectra have been acquired at each data point forming a three-dimensional

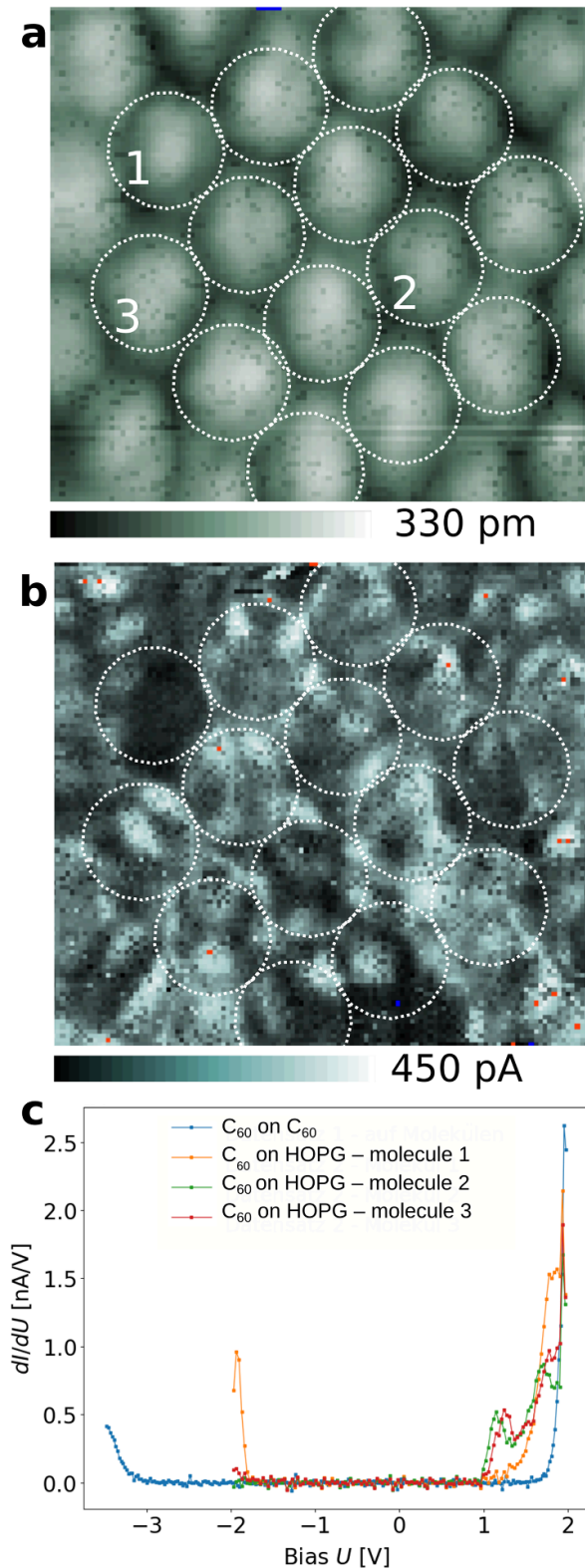


Figure 4. (a) High resolution scanning tunneling microscopy image taken on a C_{60} island on the HOPG surface. Bias voltage $U = 2$ V, tunneling current $I = 0.5$ nA. (b) Slice through scanning tunneling spectra three-dimensional data associated with image (a) at $U = 1.3$ V. In both images circles indicate a model of the position of the molecules. (c) Comparison of spectra obtained on three different molecules labeled 1, 2 and 3 in (a) with a spectrum obtained on C_{60} on a C_{60} island.

dataset. A slice through these spectra at $U = 1.3$ V is shown in figure 4(b). An image of C_{60} molecules located on HOPG directly taken from a different part of the surface associated with STS data is shown in section 5 of the supplementary material. Both, STS from C_{60} molecules located on HOPG directly and from C_{60} molecules located on a C_{60} island are shown in figure 4(c). While C_{60} molecules located on HOPG were studied between -2 V and 2 V, C_{60} molecules located on a C_{60} island were studied between -3.5 V and 2 V.

For C_{60} located on HOPG, the topographic image (figure 4(a)) clearly shows the molecular lattice and internal molecular contrast is clearly observed. However, due to the strong influence of the substrate spatial distribution of electronic orbitals on the image it was not possible to assign the orientation of the molecules. We conclude that already the lowest layer of C_{60} shows strong disorder. This disorder creates an environment where subsequent layers show local differences in strain and orientation of the molecules.

The acquisition time of 33 min was long enough to suppress noise, but short enough so that no molecular swinging is observed judging from the slice through the tunneling spectra. For swinging, we would expect horizontal steps in the image or in the spectra or both. In the lower part of the image, a tip change results in several horizontal lines. Distortions of the lattice in figures 4(a) and (b) due to the position of the molecules near the edge of an island have been limited by cutting the image. Such distortions also occur e.g. in figure 2 below the red line profile at the edge of island D and at the edges of the other islands. We expect that part of the noise in the spectra shown in figure 4(c) arises from the lower signal to noise ratio due to the small tunnel current.

In slices of the spectroscopy data such as the one shown in figure 4(b) taken at $U = 1.3$ V, the molecules all look slightly different. The spectra slices show a complicated local structure which cannot be related to molecular orientations in a simple manner. In addition we consider that the molecules might hop during the acquisition time. For rapid full rotational hopping, we would expect isotropic STS slices, for rare hops we would expect steps in the appearance of a molecule—both are not observed. Molecules could swing in a limited way at intermediate timescales, e.g. between two states, complicating the overall appearance. Indeed the structures observed in the spectra are related to the internal structure of the molecules. Since the C_{60} structure on HOPG requires a large unit cell due to the lattice constant mismatch, each molecule is located on a different position relative to the HOPG lattice. This could in addition to the molecular orientation influence the appearance of each molecule.

For closer analysis, three different molecules with different orientations were selected as examples, labeled 1–3 in figure 4(a). The spectra obtained from each molecule were averaged over rectangular areas covering the molecule and have the same spectral range from -2 V to 2 V. Three dominant molecular states, the highest occupied molecular orbital (HOMO), the lowest unoccupied molecular orbital (LUMO) and LUMO + 1 appear strongly in the spectra in particular for molecule 1 [49–51]. These molecular orbitals have been

assigned to the h_u , t_{1u} and t_{1g} molecular orbitals resp. in previous studies [52]. At negative bias we find the HOMO derived resonance located at around 2.1 V below the Fermi level, whereas at positive bias the LUMO and LUMO + 1 derived resonances are found around 1.2 ± 0.1 V for molecule 2 and 3 and 1.7 ± 0.1 V above Fermi level respectively for all three molecules. The slice at $U = 1.3$ V shown in figure 4(b) indeed shows dark contrast at the position of molecule 1 as expected from the spectrum. The HOMO–LUMO distance reveals a gap of 3.4 ± 0.1 eV for molecule 1. The energy gap is smaller than the energy gap between HOMO and LUMO of a single C_{60} molecule [53] in the gas phase (4.95 eV) but it is close to the measured HOMO–LUMO gap for solid $C_{60} \approx 3.7$ eV (reference [15]). In reference [32] it has been stated that bright and dim, i.e. differently oriented molecules show electronic states that are slightly shifted similar to what we observe here.

When C_{60} embedded in the islands is surrounded by six neighbors, the molecular states overlap with those of neighboring molecules leading to a hybridization between π orbitals of the C_{60} molecules and the value of the molecular gap changes due to the screening of charges in the electronic environment. This is in contrast to C_{60} in contact with metal surfaces; the molecular gap on HOPG is larger than that observed on metal surfaces [32, 41, 49, 50, 52, 54]. The large HOMO–LUMO gap and narrow spectral width of the molecular resonances measured for C_{60} molecules on HOPG indicates that the interaction between C_{60} and HOPG is significantly smaller than for C_{60} on various metallic substrates, implying significantly lower interfacial charge transfer. These results are in overall agreement with recent measurements on different substrates including semiconducting and insulating substrates [55, 56], revealing the efficiency of HOPG to decouple the C_{60} molecules and preserve their electronic properties.

For C_{60} located on C_{60} , the images acquired parallel to the spectroscopy look blurred possibly due to repeated swinging during the time of the measurement, see supplementary material, section 5. The spectrum shown should be considered as average information over different orientations of C_{60} . Only the HOMO state is detected at around 3.3 V below the Fermi level. We cannot deduce the molecular energy gap but we could assume that the gap is larger compared to C_{60} on HOPG taking into account that the HOMO state energy is shifted towards lower values than the ones observed for C_{60} on HOPG. While the energy gap in C_{60} on HOPG is slightly perturbed by the substrate, we expect less perturbation for C_{60} on C_{60} due to the weak intermolecular bonding. For C_{60} on C_{60} the gap should have a similar value as for the free molecule, 4.95 eV, see reference [53], in accordance with our observations.

4. Conclusion

We have studied structural and electronic properties of several molecular layers of C_{60} islands near the rotational glass transition. We observe the internal structure of C_{60} and its orientation by STM. We have focused on three different molecular layers giving us insight into the three-dimensional arrangement of the island. We found that upper and lower layers show

a 2×2 -reconstructed partially rotationally ordered hexagonal pattern whereas the layer in between exhibits a rotationally disordered pattern. There is a correlation on the orientation of layer 1 and 3, while no correlation is established between layers 1, 3 and layer 2. We can relate this difference to different bonding between the molecules. STS data confirms the disordered orientation of the molecules. Our data suggests that the orientationally disordered C_{60} structure is not fully locked but shows a relevant fraction of disorder and rotational hopping that still persists even at liquid nitrogen temperatures.

Data availability statement

The data cannot be made publicly available upon publication because the cost of preparing, depositing and hosting the data would be prohibitive within the terms of this research project. The data that support the findings of this study are available upon reasonable request from the authors.

Conflicts of interest

There are no conflicts of interest to declare.

ORCID iDs

Michael Marz  <https://orcid.org/0000-0002-8001-6488>
 Amina Kimouche  <https://orcid.org/0000-0002-4223-0782>
 Regina Hoffmann-Vogel  <https://orcid.org/0000-0003-4984-6210>

References

- [1] Binnig G, Rohrer H, Gerber C and Weibel E 1983 *Phys. Rev. Lett.* **50** 120
- [2] Paredes J I, Villar-Rodil S, Solis-Fernandez P, Martinez-Alonso A and Tascon J M D 2009 *Langmuir* **25** 5957
- [3] Otero R, Lukas M, Kelly R E A, Xu W, Laegsgaard E, Stensgaard I, Kantorovich L N and Besenbacher T 2008 *Science* **319** 312
- [4] Lichtenstein L, Heyde M and Freund H J 2012 *Phys. Rev. Lett.* **109** 106101
- [5] Pietzsch O, Kubetzka A, Bode M and Wiesendanger R 2000 *Phys. Rev. Lett.* **84** 5212
- [6] Heinze S, von Bergmann K, Menzel M, Brede J, Kubetzka A, Wiesendanger R, Bihlmayer G and Blügel S 2011 *Nat. Phys.* **7** 713
- [7] Danilov A V, Hedegard P, Golubev D S, Bjornholm T and Kubatkin S E 2008 *Nano Lett.* **8** 2393
- [8] van der Molen S J and Liljeroth P 2010 *J. Phys.: Condens. Matter* **22** 133001
- [9] Tanigaki K, Ebbesen T, Saito S, Mizuki J, Tsai J, Kubo Y and Kuroshima S 1991 *Nature* **352** 222
- [10] Hebard A, Rosseinsky M, Haddon R, Murphy D, Glarum S, Palstra T, Ramirez A and Kortan A 1991 *Nature* **350** 600
- [11] Winkelmann C B, Roch N, Wernsdorfer W, Bouchiat V and Balestro F 2009 *Nat. Phys.* **5** 876
- [12] Park H, Park J L, Lim A K L, Anderson E H, Alivisatos A P and McEuen P L 2000 *Nature* **407** 57
- [13] Bonifazi D, Enger O and Diederich T 2007 *Chem. Soc. Rev.* **36** 390

- [14] Benjamin S C *et al* 2006 *J. Phys.: Condens. Matter* **18** S867
- [15] Ohno T R, Chen Y, Harvey D E, Kroll G H, Weaver J H, Hauffler R E and Smalley R E 1991 *Phys. Rev. B* **44** 13747
- [16] Altman E I and Colton R J 1993 *Surf. Sci.* **295** 13
- [17] Rogero C, Pascual J I, Gomez-Herrero J and Baro A M 2002 *J. Chem. Phys.* **116** 832
- [18] Hoogenboom B W, Hesper R, Tjeng L H and Sawatzky G A 1998 *Phys. Rev. B* **57** 11939
- [19] Hou J G, Yang J L, Wang H Q, Li Q X, Zeng C G, Yuan L F, Wang B, Chen D M and Zhu Q S 2001 *Nature* **409** 304
- [20] Muntwiler M, Auwärter W, Seitsonen A P, Osterwalder J and Greber T 2005 *Phys. Rev. B* **71** 121402(R)
- [21] Chen C, Zheng H, Mills A, Hefflin J R and Tao C 2015 *Sci. Rep.* **5** 14336
- [22] Bozhko S I, Walshe K and Shvets I V 2019 *Sci. Rep.* **9** 16017
- [23] David W I F, Ibberson R M, Matthewman J C, Prassides K, Dennis T J S, Hare J P, Krotto H W, Taylor R and Walton D R M 1991 *Nature* **353** 147
- [24] David W I F, Ibberson R M, Dennis T J S, Hare J P and Prassides K 1992 *Europhys. Lett.* **18** 219
- [25] Burgi H B, Blanc E, Schwarzenbach D, Liu S, Lu Y J, Kappes M M and Ibers J A 1992 *Angew. Chem., Int. Ed.* **31** 640
- [26] Lu J P, Li X P and Martin R M 1992 *Phys. Rev. Lett.* **68** 1551
- [27] Laforge C, Passerone D, Harris A B, Lambin P and Tosatti E 2001 *Phys. Rev. Lett.* **87** 085503
- [28] Heiney P A, Fischer J E, McGhie A R, Romanow W J, Denenstien A M, McCauley Jr. J P, Smith A B and Cox D E 1991 *Phys. Rev. Lett.* **66** 2911
- [29] Gugenberger F, Heid R, Meingast C, Adelman P, Braun M, Wühl H, Haluska M and Kuzmany H 1992 *Phys. Rev. Lett.* **69** 3774
- [30] Meingast C and Gugenberger F 1993 *Mod. Phys. Lett. B* **07** 1703–24
- [31] Schelkacheva T I, Tareyeva E E and Chitchev N M 2007 *Phys. Rev. B* **76** 195408
- [32] Grobis M, Lu X and Crommie M F 2002 *Phys. Rev. B* **66** 161408(R)
- [33] Burke S A, Mativetsky J M, Hoffmann R and Grütter P 2005 *Phys. Rev. Lett.* **94** 096102
- [34] Hoffmann-Vogel R 2018 *Rep. Prog. Phys.* **81** 016501
- [35] Wang H, Zeng C, Wang B, Hou J G, Li Q and Yang J 2001 *Phys. Rev. B* **63** 085417
- [36] Yuan L-F, Yang J, Wang H, Zeng C, Li Q, Wang B, Hou J G, Zhu Q and Chen D M 2003 *J. Am. Chem. Soc.* **125** 169
- [37] Reddy C D, Yu Z G and Zhang Y-W 2015 *Sci. Rep.* **5** 12221
- [38] Marz M, Sagisaka K and Fujita D 2013 *Beilstein J. Nanotechnol.* **4** 406
- [39] Seydel E, Hoffmann-Vogel R and Marz M 2019 *Nanotechnology* **30** 025703
- [40] Ulbricht H, Moos G and Hertel T 2003 *Phys. Rev. Lett.* **90** 095501
- [41] Lu X, Grobis M, Khoo K H, Louie S G and Crommie M F 2003 *Phys. Rev. Lett.* **90** 096802
- [42] Stipe B C, Rezaei M A and Ho W 1998 *Science* **279** 1907
- [43] Frauhammer T, Gerhard L, Edelmann K, Lindner M, Valášek M, Mayor M and Wulfhekel W 2021 *Phys. Chem. Chem. Phys.* **23** 4874
- [44] Ramirez A P 1994 *Annu. Rev. Mater. Sci.* **24** 453
- [45] Cepek C, Goldoni A and Modesti S 1996 *Phys. Rev. B* **53** 7466
- [46] Larsson J A, Elliott S D, Greer J C, Repp J, Meyer G and Allenspach R 2008 *Phys. Rev. B* **77** 115434
- [47] Shin H, O'Donnell S E, Reinke P, Ferralis N, Schmid A K, Li H I, Novaco A D, Bruch L W and Diehl R D 2010 *Phys. Rev. B* **82** 235427
- [48] Copley J R D *et al* 1992 *Physica B* **180–181** 706
- [49] Schull G, Neél N, Becker M, Kröger J and Berndt R 2008 *New J. Phys.* **10** 065012
- [50] Schulze G, Franke K J and Pascual J I 2008 *New J. Phys.* **10** 065005
- [51] Grobis M, Wachowiak A, Yamachika R and Crommie M F 2005 *Appl. Phys. Lett.* **86** 204102
- [52] Silien C, Pradhan N A, Ho W and Thiry P A 2004 *Phys. Rev. B* **69** 115434
- [53] Dresselhaus M S, Dresselhaus G and Eklund P C 1996 *Science of Fullerenes and Carbon Nanotubes* (Academic)
- [54] Liu C, Qin Z, Chen J, Guo Q, Yu Y and Cao G 2011 *Chem. Phys.* **134** 044707
- [55] Sun K and Kawai S 2021 *Phys. Chem. Chem. Phys.* **23** 5455
- [56] Liu Z, Sun K, Li X, Li L, Zhang H and Chi L 2019 *J. Phys. Chem. Lett.* **10** 4297